Editor's Summary

A Screening Room for Cerebral Malaria Drugs

Smart-phone retailers claim that their device brings the cinema to you. Yet, there's something to be said for ambiance: A blockbuster film delivers more effective entertainment when screened in high-def surround sound versus on a 6-inch screen in a jammed subway car. Screening new drugs is no different. Although in vitro drug-screening models are convenient, it's attention to pathophysiological details that creates an informative and predictive drug-screening platform. Achtman *et al.* now repurpose a mouse model of experimental cerebral malaria (ECM) to screen for adjuvant therapy against severe malaria.

Although first-line antimalarial drugs may control parasitemia, they do little to quell the inflammation that leads to seizures, coma, and long-term sequelae in patients with severe malaria. The authors hypothesized that innate defense regulator (IDR) peptides—host-derived signaling molecules that modulate the innate immune system—would serve as anti-inflammatory adjuvant therapy for ECM in combination with first-line drugs. The authors adapted the murine *Plasmodium berghei* ANKA ECM model to serve as a preclinical drug-screening platform by combining antimalarial drug intervention in established malarial infections with iterative mouse-human bioinformatic analysis. When co-administered with first-line antimalarial drugs, the IDR peptide down-regulated inflammatory networks and improved mouse survival. If these data translate to humans, IDR peptides could provide an anti-inflammatory adjuvant therapy for severe malaria and perhaps other infectious diseases.

A complete electronic version of this article and other services, including high-resolution figures, can be found at:
http://stm.sciencemag.org/content/4/135/135ra64.full.html

Supplementary Material can be found in the online version of this article at:
http://stm.sciencemag.org/content/suppl/2012/05/21/4.135.135ra64.DC1.html

Information about obtaining **reprints** of this article or about obtaining **permission to reproduce this article** in whole or in part can be found at:
http://www.sciencemag.org/about/permissions.dtl

MALARIA

Effective Adjunctive Therapy by an Innate Defense Regulatory Peptide in a Preclinical Model of Severe Malaria

Ariel H. Achtman,[1,2]* Sandra Pilat,[1,2]* Charity W. Law,[1,2] David J. Lynn,[3,4,5] Laure Janot,[3] Matt L. Mayer,[3] Shuhua Ma,[3] Jason Kindrachuk,[3] B. Brett Finlay,[6] Fiona S. L. Brinkman,[4] Gordon K. Smyth,[1,7] Robert E. W. Hancock,[3] Louis Schofield[1,2†]

Case fatality rates for severe malaria remain high even in the best clinical settings because antimalarial drugs act against the parasite without alleviating life-threatening inflammation. We assessed the potential for host-directed therapy of severe malaria of a new class of anti-inflammatory drugs, the innate defense regulator (IDR) peptides, based on host defense peptides. The *Plasmodium berghei* ANKA model of experimental cerebral malaria was adapted to use as a preclinical screen by combining late-stage intervention in established infections with advanced bioinformatic analysis of early transcriptional changes in co-regulated gene sets. Coadministration of IDR-1018 with standard first-line antimalarials increased survival of infected mice while down-regulating key inflammatory networks associated with fatality. Thus, IDR peptides provided host-directed adjunctive therapy for severe disease in combination with antimalarial treatment.

INTRODUCTION

Clinically severe or life-threatening malaria presents a global health challenge. Clinical symptoms include seizures and coma, with long-term neurological and physical sequelae in survivors. Diverse organ-specific or systemic disease syndromes in *Plasmodium falciparum* infection are thought to represent the end-stage processes of parasite sequestration in local sites and inflammatory cascades initiated by pathogen toxins. The only effective treatment for clinically severe malaria is parenteral administration of antimalarial drugs (*1*), which control parasitemia but do little to reverse pathophysiological processes already under way in the brain or other organs.

Various adjunctive therapies assessed in preclinical models or small clinical trials (*1*) either were ineffective or provided contradictory outcomes. The rational development of supportive or adjunctive therapies is hindered by both lack of clarity as to underlying pathologic mechanisms in severe malaria and a failure to develop appropriate preclinical screens. The relevance of the murine *Plasmodium berghei* ANKA experimental cerebral malaria (ECM) model to human disease has been extensively debated (*2–8*). Differences in opinion revolve around two issues, namely, the relative contributions to these syndromes of parasite sequestration and host inflammation, and the reliance on early-stage rather than late-stage interventions in exploiting the model (*2–8*). In addition to extensive data linking proinflammatory responses to malaria disease states (*9–13*), unbiased and hypothesis-driven gene association studies have identified immune regulatory and effector loci as a major ontological class of mutations associated with susceptibility and resistance to human severe malaria (*14*). These findings justify research into anti-inflammatory drugs for the supportive therapy of severe malaria.

Host defense peptides (such as defensins or cathelicidins) and their synthetic innate defense regulator (IDR) analogs modulate innate immunity. Their modes of action include chemokine secretion, cell differentiation, and the suppression of potentially harmful inflammatory responses (*15–17*). In addition, they enhance adaptive immune responses (*18*). These multiple modes of action make host defense peptides attractive tools in combating a multifactorial syndrome such as cerebral malaria (CM). Accordingly, we sought to use the ECM system to assess late-stage intervention in combination with first-line antimalarial treatment as a preclinical screen for the therapeutic efficacy of IDR-1018 as a host-directed therapy and adjunctive treatment for severe malaria. Adjunctively administered IDR-1018 was significantly more protective against late-stage infection than antimalarial treatment alone, and this was linked to reduced inflammation.

RESULTS

Prophylactic administration of IDR-1018 peptide reduced the incidence of ECM

Peptide IDR-1018, based loosely on Bac2a (fig. S1A), the linear form of the bovine host defense peptide bactenecin, was selected for its broad anti-inflammatory capabilities. IDR-1018 suppressed lipopolysaccharide (LPS)–induced production of tumor necrosis factor–α (TNF-α) in vitro and protected mice from *Staphylococcus aureus* infection (fig. S1B). The peptide's potent ability to modulate inflammatory immune responses and its low toxicity profile indicated its potential as an adjunctive therapy for malaria treatment. IDR-1 [fig. S1A (*16*)], a less potent immune modulator, was used as a control.

In the *P. berghei* ANKA/C57BL/6 model of ECM, 90 to 100% of mice die from inflammatory processes in the brain about 6 to 8 days

[1]Walter and Eliza Hall Institute for Medical Research, 1G Royal Parade, Parkville, Victoria 3052, Australia. [2]Department of Medical Biology, University of Melbourne, Parkville, Victoria 3010, Australia. [3]Centre for Microbial Diseases and Immunity Research, University of British Columbia, Vancouver, British Columbia V6T 1Z4, Canada. [4]Department of Molecular Biology and Biochemistry, Simon Fraser University, 8888 University Drive, Burnaby, British Columbia V5A 1S6, Canada. [5]Animal and Bioscience Research Department, AGRIC, Teagasc, Grange, Dunsany, County Meath, Ireland. [6]Michael Smith Laboratories, University of British Columbia, Vancouver, British Columbia V6T 1Z4, Canada. [7]Department of Mathematics and Statistics, University of Melbourne, Parkville, Victoria 3010, Australia.
*These authors contributed equally to this work.
†To whom correspondence should be addressed. E-mail: schofield@wehi.edu.au

after infection, with comparatively low parasite burdens (~10 to 15%). We first tested intraperitoneal and intravenous prophylactic administration of IDR-1018 (Fig. 1A). The intraperitoneal treatment with IDR-1018 peptide was not protective, with 100% of mice in this group dying of ECM at rates comparable to those of saline-injected controls (93%) (Fig. 1B). However, 56% of intravenous IDR-1018–treated mice were protected (Fig. 1B, $P = 0.0019$). Although mice were treated with IDR-1018 only up to day 9 of infection, there was no late recurrence of ECM symptoms.

Drugs can protect against ECM by reducing either parasitemia or pathology. Alterations in reticulocyte levels may have downstream effects on parasitemia because they are the preferred invasion target for *P. berghei* in late-stage infections. Reticulocyte levels were significantly ($P = 0.004$) higher in IDR-1018 intravenously treated mice than in saline-treated animals on day 3 after infection (Fig. 1C), but this effect did not persist. Moreover, IDR-1018 treatment did not affect parasitemia (Fig. 1D), suggesting that the peptide acts in a host-directed manner.

IDR-1018 adjunctive treatment increased protection from ECM

IDR-1018 was tested in an adjunctive treatment regimen (Fig. 2). To approximate the clinical setting, where treatment occurs after admission, we commenced intravenous IDR-1018 treatment in combination with antimalarial drugs on day 4 of infection, when the animals manifested peripheral parasitemias of 3 to 6% (Fig. 2A). All saline-treated mice developed fatal ECM by day 7 after infection (Fig. 2, B and C). Treatment of an established infection with IDR-1018 without antimalarials neither slowed down nor prevented ECM development (Fig. 2B). Pyrimethamine-chloroquine antimalarial treatment of established infections protected only 41% of mice from ECM. Protection

from ECM was significantly ($P = 0.034$) boosted to 68% by adjunctive treatment with IDR-1018 peptide together with antimalarial drugs (Fig. 2C). In contrast, the control peptide IDR-1 (16) failed to protect in this model, even though it exhibited some protection prophylactically (Fig. 2D).

Malaria infection and treatment with IDR-1018 created distinct transcriptional profiles

Microarray analyses were performed to provide mechanistic insights into the protective effect of IDR-1018 against ECM. The microarrays compared nine IDR-1018 intravenously treated, infected mice (IDR-1018–treated infected) with three saline intravenously treated, infected mice (saline-treated infected) and three uninfected untreated mice (controls). In ECM, the spleen is the origin of immunopathological processes and the brain is the site of terminal events. To detect both early-onset causal processes and pathology, we administered IDR-1018 prophylactically and harvested spleens and brains on day 3 of infection (Fig. 3A). In our past ECM experiments, a group size of three has produced consistent microarray profiles (19), but we expected high transcriptional diversity in the IDR-1018–treated infected group because of incomplete penetrance of the protective phenotype. We compensated by tripling the size of the IDR-1018–treated infected group. The efficacy of peptide treatment in this experiment was confirmed by tracking the ECM outcome for mice infected in parallel with the animals used for microarray analysis. All of the saline-treated infected mice died of ECM by day 7 after infection, whereas 44% of the IDR-1018–treated infected animals were protected from ECM (Fig. 3A).

An unsupervised plot was used to display the overall relatedness of the 15 microarray expression profiles for each tissue. For each pair of samples, the leading fold change was computed as the typical $\log_2$ fold change of the 500 most discrepant genes between those samples. Then,
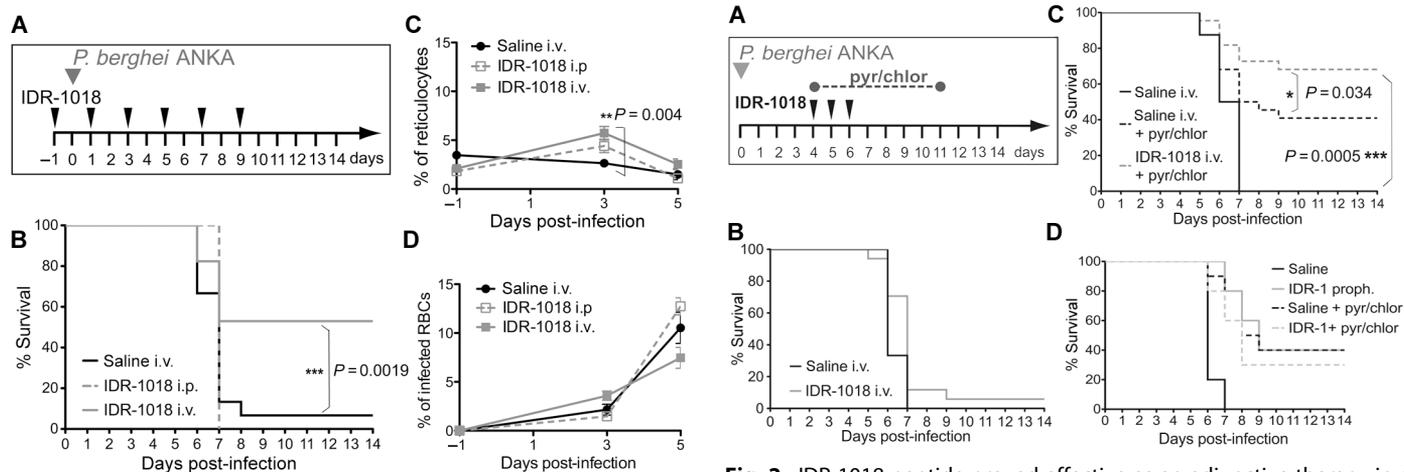
Fig. 1. Intravenously delivered IDR-1018 peptide fully protected 56% of mice from ECM. (**A**) Peptide and parasite administration. (**B**) Survival was improved after IDR-1018 intravenous (i.v.) treatment compared to saline i.v. controls (17 compared to 15 mice combined from two independent experiments, $P = 0.0019$), but not after IDR-1018 intraperitoneal treatment compared to saline intraperitoneal controls ($n = 8$ per group, $P > 0.5$). (**C** and **D**) Reticulocyte (C) and parasitemia (D) levels in peripheral blood from one experiment ($n = 8$ per group) are shown as averages ± SEM. Only statistically significant P values for treated compared to untreated mice are shown (all panels). RBCs, red blood cells.

Fig. 2. IDR-1018 peptide proved effective as an adjunctive therapy in a preclinical model. (**A**) Peptide, pyrimethamine and chloroquine (pyr/chlor), and parasite administration. (**B**) Eighteen mice received adjunctive IDR-1018 i.v. and 12 mice saline i.v. (combined from two experiments, $P = 0.15$). (**C**) Twenty-two mice received IDR-1018 i.v. and oral antimalarials, 22 mice saline i.v. and oral antimalarials, and 8 mice saline i.v. only (combined from two experiments, $P = 0.0005$ for IDR-1018 i.v. + pyr/chlor compared to saline i.v. and $P = 0.034$ for IDR-1018 i.v. + pyr/chlor compared to pyr/chlor). (**D**) The control peptide IDR-1 was given i.v. prophylactically (proph.) as in Fig. 1A or adjunctively with antimalarials as in (A) (10 mice per group).
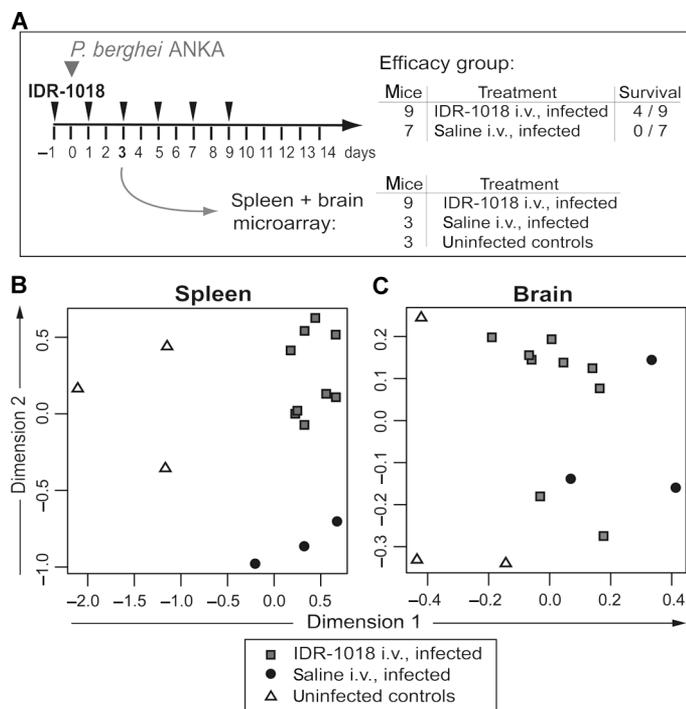
Fig. 3. IDR-1018 treatment had a transcriptional impact during infection. (**A**) Prophylactic peptide administration and infection protocol. The efficacy cohort was tracked until day 14, whereas all microarray organs were harvested 3 days after infection. (**B** and **C**) Multidimensional scaling plots show relationships between the transcriptional profiles of all samples from either spleen (B) or brain (C). Dimensions 1 and 2 represent distances between samples, which can be interpreted as average $\log_2$ fold change for the 500 genes that best distinguish each pair of samples.

multidimensional scaling was used to construct a two-dimensional plot of the samples in which the distances between points correspond to leading $\log_2$ fold changes. For the spleen, the three experimental groups formed distinct clusters, indicating that both infection and amelioration by the IDR-1018 peptide have transcriptional effects as early as day 3 of infection (Fig. 3B). For the brain samples from the same time point, the transcriptional differences were smaller, consistent with the cellular shift from spleen to brain during the course of infection. Although the two infected brain groups were distinct from the uninfected controls, the group treated with IDR-1018 partially overlapped the saline-treated group (Fig. 3C).

Comparing the transcriptional profiles for the spleens of IDR-1018–treated with saline-treated infected mice revealed 69 down-regulated and 353 up-regulated genes with fold change of >1.5 and false discovery rate (FDR) of <0.1. Pathway analysis of IDR-1018–treated compared to saline-treated infected spleens revealed the down-regulation of a network of immune response genes linked by the inflammatory cytokines TNF-α and interferon-γ (IFN-γ) (the latter not differentially expressed) (Fig. 4A). These included inflammatory cytokine and chemokine genes (*IL-1, IL-1RN, CCL3/MIP-1α,* and *CCL4/MIP-1β*) as well as other genes associated with cellular migration [*PLAU* and *SPHK1* (up-regulated)]. Additionally, genes involved in T cell activation [*CD86, CD69, Gm6273/Trbv1* (T cell receptor βV), *microRNA miR-101a, CD274/PD-L1, HSH2D/ALX,* and *CD27*], macrophage activity (*OASL, SLC11a1, PLAU, CCL3/MIP-1α,* and *CCL4/MIP-1β*), and antigen presentation (*HLA-DQB1/H2-Ab1,*

H2-Q8, and *CD200*) were also down-regulated. Of these genes, 83% were up-regulated in the comparison between saline-treated infected and control mice, consistent with IDR-1018 treatment counterregulating (suppressing) transcriptional processes activated by infection.

In contrast, a network of genes associated with erythropoiesis was up-regulated in the IDR-1018–treated compared to the saline-treated infected spleens (Fig. 4B). This included six of the eight genes for key enzymes in heme biosynthesis as well as central regulators of erythropoiesis such as *GATA-1* and *EPO-R. SOCS3* and *HMAG1* were the only examples of these genes differentially expressed (up-regulated) between saline-treated infected and uninfected spleens. Further up-regulated genes fell into the functional categories of cell cycle, DNA replication, and DNA repair. Pathways regulating the G_2-M and G_1-S transitions of the cell cycle and DNA repair in response to cell stress or injury were statistically overrepresented in network analysis (summarized in Fig. 4C). Other statistically overrepresented pathways included metabolic pathways related to pyrimidine metabolism and glutathione metabolism. ABC (adenosine triphosphate–binding cassette) transporters were also overrepresented.

To address the incomplete penetrance of survival in IDR-1018–treated infected mice, we examined variability among transcriptional profiles of the nine treated mice. To focus on genes relevant to ECM, we undertook a linear discriminant analysis to distinguish the uninfected from the saline-treated infected expression profiles. This analysis produced discriminant functions (or metagenes), weighted averages of the individual genes, that best separated the uninfected and saline-treated infected groups. All the expression profiles, including those for IDR-1018–treated mice, were displayed in a scatterplot according to the first two discriminant functions. Applied to splenic expression profiles, this semisupervised analysis showed that the IDR-1018–treated mice were intermediate between and more heterogeneous than either the uninfected or the saline-treated infected groups (Fig. 5A). Genes that received positive weights in the first discriminant function, and hence were associated with ECM, were dominated by IFN-γ and a range of genes associated either with IFN-γ (*GBP2, WARS, Irgm1, IL-7, Serpina3f,* and *Nlrc5*) or both type I and type II IFNs (*Ifi205, Irf1, Gbp10, Oas1g,* and *STAT1*) (Table 1). The second discriminant function was almost entirely determined by IFN-γ.

In the brain transcriptome, the only gene differentially expressed between infected IDR-1018–treated and saline-treated mice was *Hbb-b1* (up-regulated), which encodes hemoglobin B1. This limited differential expression was consistent with the poor separation of the groups in the brain multidimensional scaling plot (Fig. 3C). To focus more closely on the ECM phenotype, we examined a set of genes that, according to three published studies (19–21), have altered brain expression in *P. berghei*–infected, ECM-susceptible mice early in infection (see Materials and Methods). Each gene in the set was classed as either positively or negatively associated with ECM (table S1). Collectively, these genes were used to represent the transcriptional signature of the ECM phenotype. The behavior of the signature was examined using a gene set test method (ROAST) that assesses the significance of changes in the ECM signature as a unit (22).

With this statistically powerful method, it became possible to identify collective trends of co-regulated genes regardless of individual *P* values. We tested for changes in this signature between the brain expression profiles of control, IDR-1018–treated infected, and saline-treated infected mice (Fig. 5B). The ECM transcriptional signature was significantly increased in brains from both saline-treated infected
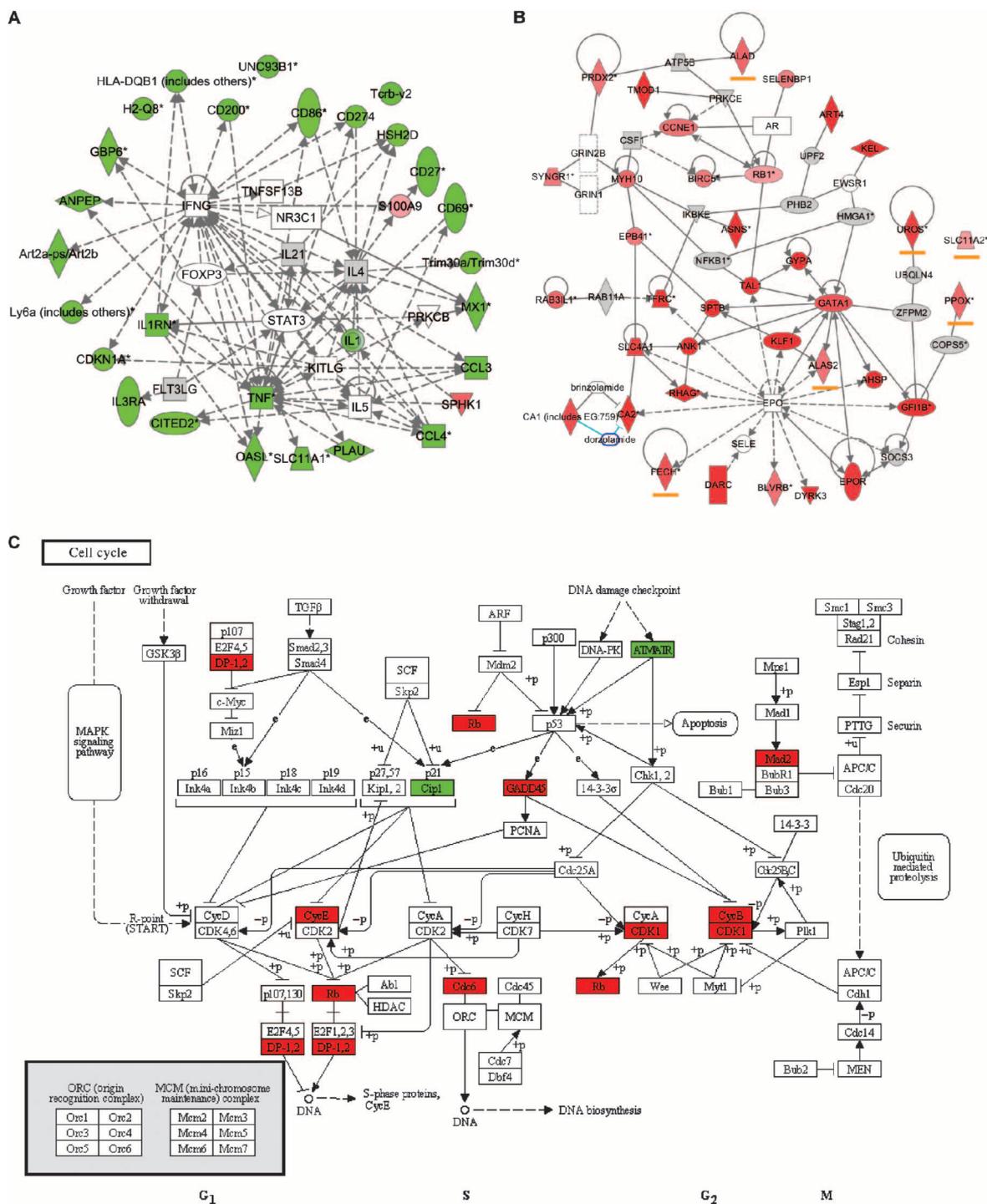
Fig. 4. IDR-1018 regulated gene networks of inflammation, cell cycle, and DNA repair. Red genes were up-regulated and green genes were down-regulated in the spleens of IDR-1018–treated compared with saline-treated mice on day 3 of *P. berghei* ANKA infection. For all networks, differential gene expression was defined as fold change of >1.5 and FDR of <0.1. (**A** and **B**) Networks were designed in IPA. Color intensity signifies the degree of regulation, and shapes represent classes of encoded proteins. Gray genes were not differentially expressed and white genes were not rep-

resented in the uploaded data set, but their connectivity was determined through network analysis. Solid lines represent direct interactions, and dotted lines represent indirect interactions. Genes not linked by lines fit these networks functionally but had no stored interactions with other displayed genes. (A) Network of differentially expressed genes associated with immune responses. (B) Network of differentially expressed genes associated with erythropoiesis. Genes involved in heme biosynthesis are underlined orange. (**C**) KEGG diagram (*47, 48*) of the cell cycle, with gene expression values overlaid.

Fig. 5. The IDR-1018–treated infected group was transcriptionally diverse. (**A**) Linear discriminant function plot showing the location of IDR-1018–treated infected mice in relationship to the saline-treated infected group and uninfected controls. The plot displays the first and second discriminant functions (that distinguished the saline-treated infected from uninfected spleens) for all mice. (**B**) Differences in collective regulation of ECM-associated genes were studied using gene set tests. Barcode plots depict genes up-regulated (red) or down-regulated (blue) in published microarray analyses of ECM brains. This was overlaid onto all the differential expression results from the microarrays in this study; genes were ranked left to right by moderated t statistics in this study, with red and blue shading respectively representing up- and down-regulation. Biased clustering of up-regulated genes (red) toward the left of the barcode plot and of down-regulated genes (blue) toward the right signifies non-random distribution of the ECM signature concordant with the current study. (**C**) P values are given for ROAST analysis of each individual IDR-1018–treated infected mouse brain compared to the group of saline-treated infected (STI) mice. (**D**) Gene set testing for receptors for inflammatory cytokines and chemokines. Fewer genes are marked in the brain because of filtering of nonexpressed genes.
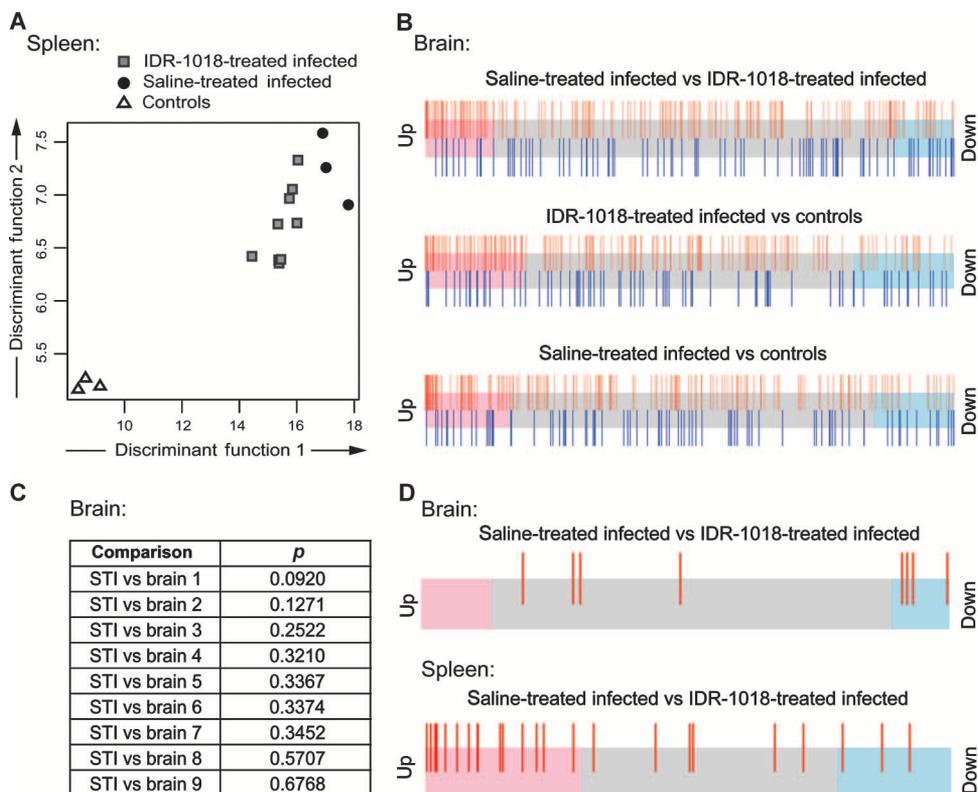
($P = 0.0091$) and IDR-1018–treated infected mice ($P = 0.0446$) relative to uninfected controls. The ECM signature also tended to be higher in saline-treated infected than in IDR-1018–treated infected mouse brains, that is, the signature appeared to be suppressed by IDR-1018 treatment ($P = 0.0683$). There was considerable variation when comparing individual IDR-1018–treated mice to the saline-treated infected group, with brains from mice 1 and 2 showing the greatest differential expression of ECM-associated genes (Fig. 5C). Together with the spleen results (Fig. 5A), these data reveal high transcriptional variability in the IDR-1018–treated infected group.

To elucidate the anti-inflammatory function of IDR-1018 in ECM, we examined the expression of receptors for inflammatory cytokines and chemokines (Fig. 5D and table S2). This gene set was significantly ($P = 0.006$) up-regulated in the saline-treated infected compared to IDR-1018–treated infected spleens (that is, down-regulated by IDR-1018), but not in the brain. Network analysis of transcriptional changes induced by IDR-1018 in LPS-stimulated human CD14+ monocytes (fig. S2A) revealed targeting of major signaling pathways. These included the nuclear factor κB (NF-κB), mitogen-activated protein kinase, phosphatidylinositol 3-kinase, and Src family kinase pathways and key downstream transcription factors for TNF-α (*NF-κB1*, *NF-κB2*, and *REL*) and IFN-γ signaling (*STAT1*). Gene set testing of the genes involved in this signaling network in the day 3 ECM expression data (fig. S2B) revealed that IDR-1018 modulated this gene set in a comparable fashion in the context of murine malaria ($P = 0.0001$ for the comparison of IDR-1018–treated infected and saline-treated infected mice) in the spleen, but not in the brain.

IDR-1018 inhibited secretion of the inflammatory mediators identified by microarrays

To validate the anti-inflammatory effect of IDR-1018 observed in the microarrays, we separately stimulated murine bone marrow–derived macrophages (BMDMs) with the Toll-like receptor 4 (TLR4) agonist, bacterial LPS, in the presence and absence of IFN-γ, the TLR2 agonist PAM3CSK4, and the TLR9 agonist CpG 2395. These TLR pathways correspond to those activated by parasite glycosylphosphatidylinositol toxin and hemozoin (12). The TLR agonists stimulated secretion of the inflammatory cytokines/chemokines TNF-α, CCL3/MIP-1α, and CCL4/MIP-1β starting at either 4 or 8 hours, and this was sustained over 24 hours. The addition of IDR-1018 at 100 μg/ml completely inhibited the secretion of TNF-α, CCL3/MIP-1α, and CCL4/MIP-1β induced by LPS, LPS/IFN-γ, and CpG 2395 (only TNF-α was tested for this stimulus), as well as partially reducing the TNF-α response to PAM3CSK4 (Fig. 6, A to E). IDR-1018 still exerted its dampening activity when added up to 4 hours after the inflammatory stimulus (Fig. 6F).

DISCUSSION

This study demonstrated the efficacy of adjunctively administered IDR peptide IDR-1018 against ECM. With the aid of advanced bioinformatic analyses, we explored this model for more effective preclinical screening of potential adjunctive therapies for human CM. Immune interventions frequently offer 100% protection against ECM if given prophylactically, but most are not effective against established

Table 1. The top 40 probes contributing to the discriminant function that distinguished saline-treated infected from uninfected expression profiles in the spleen. Weights represent the contribution of each probe to the discriminant score. Positive weights indicate positive correlation with infection, whereas negative weights indicate negative correlation. Note that multiple microarray probes can map to the same gene.

Gene symbol	Probe ID	ArrayAddress ID	Weight
Ifi205	ILMN_2437969	7400528	0.355
Gbp2	ILMN_3047389	6860600	0.302
Irf1	ILMN_2649067	3400288	0.234
Irf1	ILMN_2649068	5820609	0.221
Ifi205	ILMN_1245200	1660184	0.217
Gm12250	ILMN_2534151	1400220	0.207
NA	ILMN_2567962	4850689	0.185
Limch1	ILMN_2628603	2510382	−0.179
NA	ILMN_2552783	3780474	0.175
Ifit2	ILMN_2981167	5270398	−0.175
Wars	ILMN_1254157	2350397	0.170
Wars	ILMN_3156343	1470176	0.169
Wars	ILMN_3077377	650167	0.160
Irf1	ILMN_2624100	1190088	0.155
Gm12185	ILMN_2847773	4210349	0.149
Itgb5	ILMN_2663613	1770152	−0.141
NA	ILMN_1246194	3460504	0.140
Tsc22d3	ILMN_3150811	6840382	−0.134
Irgm1	ILMN_1234539	5820608	0.133
Ifng	ILMN_2685712	2850092	0.120
NA	ILMN_2771766	1990221	−0.115
Gbp10	ILMN_2808485	1500246	0.111
NA	ILMN_1233449	2190133	0.107
Ifit3	ILMN_2944666	7510020	−0.102
Il7	ILMN_2630852	1110296	−0.101
E130203B14Rik	ILMN_1246821	5420445	−0.098
Hmgcs2	ILMN_1216322	6280392	−0.097
Ifit2	ILMN_2981169	360041	−0.089
Igfbp3	ILMN_1219335	1820601	−0.089
NA	ILMN_1223311	3890292	−0.088
Trim30d	ILMN_2695412	4390576	0.087
Serpina3f	ILMN_2742861	4540082	−0.085
Cdkn1c	ILMN_2708203	4570451	−0.083
Oas1g	ILMN_2628822	130598	−0.083
Htra3	ILMN_2718401	780546	−0.081
Nlrc5	ILMN_3161790	520040	0.079
Stat1	ILMN_2593196	4260528	0.076
Mmp13	ILMN_2737685	5690131	−0.075
Ifit3	ILMN_1230458	670670	0.074
Mx2	ILMN_1239219	520278	−0.074

infections. A critical evaluation of the *P. berghei* ANKA ECM model resulted in recommendations to improve the model's utility (*2–8*): (i) use the ECM model primarily as a preclinical screen for drug development, (ii) focus on adjunctive therapies in combination with antimalarials, (iii) late-stage rather than early-stage treatment, and (iv) iterative approaches alternating between humans and mice. The current study implemented all recommendations by using IDR-1018 adjunctively with antimalarial treatment of established infections, iteratively deploying in the mouse model a drug selected for ability to modulate inflammatory responses in human peripheral blood mononuclear cells (PBMCs), and confirming comparable modes of action in murine cells in vitro. The IDR class of peptides is being optimized further in mouse models, and the first IDR peptide has completed phase 1 clinical trials (*23*).

IDR-1018 treatment suppressed transcriptional pathways of antigen processing, macrophage activity, cell migration, and T cell activation in the spleen, consistent with the known splenic priming of parasite-specific CD8+ and CD4+ T cells contributing to brain pathology in ECM (*12, 24, 25*). Elucidating the relative importance of these processes in IDR-1018–mediated alleviation of ECM is difficult because ECM results from a complex cellular network (*12*). We hypothesize that IDR-1018 alleviates brain pathology by down-regulating inflammatory cytokine and chemokine expression, thereby reducing splenic production of highly activated inflammatory T cells and natural killer cells. Proinflammatory cytokines are proposed to mediate pathology in human severe malaria (*9, 10*), and increased levels of inflammatory cytokines in the plasma and cerebrospinal fluid are strongly associated with severe disease (*13, 26*), as are promoter polymorphisms in cytokine genes (*14*).

Transcriptional analyses and in vitro stimulation with TLR agonists showed IDR-1018 reducing production and effects of the proinflammatory cytokines IFN-γ and TNF-α and chemokines CCL3/MIP-1α and CCL4/MIP-1β. These have all been implicated in severe malaria in humans and mice, but no individual molecule is identified as a key regulator in all settings. Neutralization of IFN-γ reduces the incidence of ECM and prevents TNF-α overproduction (*27*). In humans, heterozygosity for an IFN-γR1 polymorphism was associated with a lower incidence of CM and malaria fatality (*28*). TNF-α is proposed as a critical mediator of disease (*9, 10*), and several studies report associations between TNF-α and CM (*29*) or severe malaria (*30, 31*). However, TNF-α–deficient mice remain susceptible to ECM (*32*), and in a clinical trial, treatment with a monoclonal anti–TNF-α antibody did not protect from CM and exacerbated neurological sequelae (*33*). Both IFN-γ and TNF-α were also associated with reduced risk of morbidity in longitudinal cohort studies (*34, 35*).

A role for inflammatory chemokines in severe malaria has only recently been recognized (*26*), and high levels of MIP-1α and MIP-1β have been linked to human CM (*26, 36, 37*) and severe malaria in mice (*38*). Thus, the network and linearized discriminant function analyses used here may represent important tools in the use of *P. berghei* ANKA ECM as a preclinical screen. The ability of a drug candidate such as IDR-1018 to affect a range of functionally related inflammatory mediators increases the likelihood that the effect will translate to human CM.

Transcriptional analyses allowed dissection of ECM development at an extremely early stage, well before mice manifest physical symptoms. The bioinformatic tools ROAST and linear discriminant function analysis enabled discrimination of the transcriptional variability in the IDR-1018–treated group of infected mice. Although changes in gene expression associated with ECM were dampened in all IDR-1018–treated mice, the variations between individual mice could be
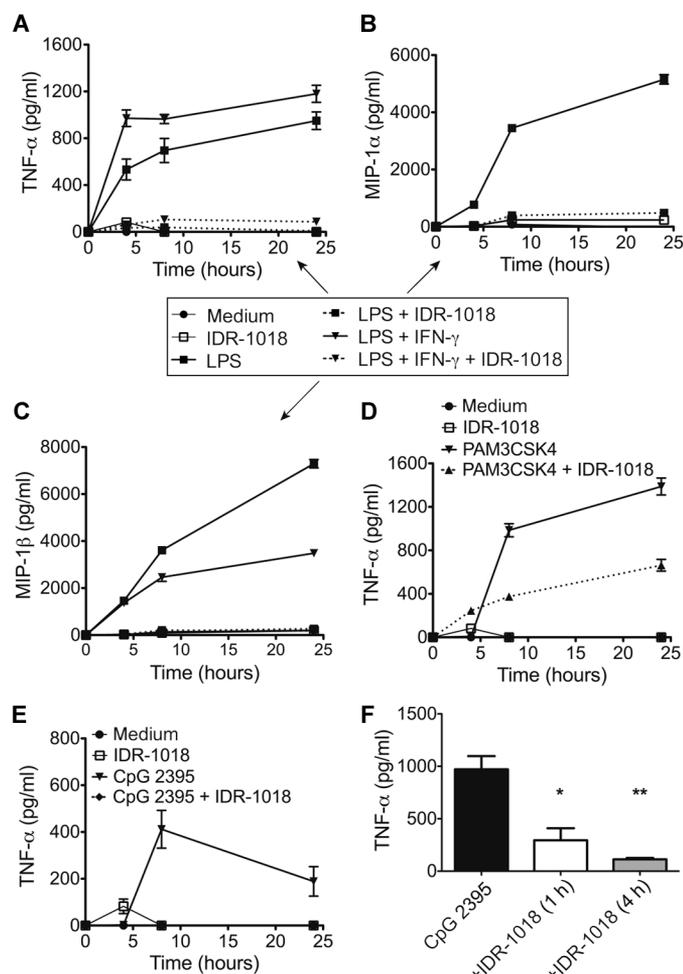
Fig. 6. IDR-1018 exerted an in vitro anti-inflammatory effect on TLR agonist–stimulated BMDMs. Cells were stimulated with TLR ligands with or without IDR-1018. (**A** to **E**) Secreted TNF-α (A, D, and E), MIP-1α (B), and MIP-1β (C) in supernatants at 4, 8, and 24 hours was measured by enzyme-linked immunosorbent assay. BMDMs were stimulated with (A to C) LPS alone or, in combination with IFN-γ, with (D) PAM3CSK4 or (E) CpG 2395. Averages from six wells ± SEM are shown and were representative of three independent experiments. Comparing stimulation with IDR-1018 + TLR agonist (or + TLR agonist + IFN-γ) to the stimulant alone, $P < 0.0001$ for all 8- and 24-hour time points except TNF-α after 8-hour LPS ($P = 0.0014$), MIP-1α after 24-hour LPS + IFN-γ ($P = 0.0002$), TNF-α after 8-hour CpG 2395 ($P = 0.0038$), and TNF-α after 24-hour CpG 2395 ($P = 0.030$). (**F**) Splenocytes from three mice (representative of two experiments) were stimulated with CpG 2395, followed by IDR-1018 and supernatant harvesting at 24 hours. *$P < 0.05$; **$P < 0.01$.

associated with differences in survival outcome. Studying coordinate regulation of a linked gene set is far more powerful than examining flux in individual genes. It is possible that future analysis of different time points of infection would further increase precision, allowing tracking of all stages of pathogenesis.

The up-regulation of genes associated with erythropoiesis in the spleens of IDR-1018–treated infected mice correlated with a transient increase in peripheral reticulocyte numbers and enhanced expression of Hbb-b1 in the brain, attributable to increased peripheral erythro-

blasts. The increase in erythropoiesis may have contributed to the overrepresentation of cell cycle and DNA replication genes. Moderate suppression of erythropoietic transcription in the spleen was observed on day 3 after infection with 10^6 P. berghei ANKA–infected erythrocytes and was pronounced by day 5 (19), so the effect of IDR-1018 treatment on erythropoiesis could become a counterregulatory force in adjunctive treatment.

In addition to regulating erythropoiesis, erythropoietin (EPO) inhibits the induction of proinflammatory TNF-α and nitric oxide synthase by blocking the activation of NF-κB p65 (39). EPO treatment in the inflammatory disease model of experimental colitis significantly reduces transcription of proinflammatory cytokines and alleviates disease. EPO protects mice from P. berghei ANKA–induced ECM (40, 41). High levels of EPO are also associated with protection from the neurological sequelae of CM in African children (42). Thus, EPO may act independently in a tissue-protective manner in the brains of IDR-1018–treated infected mice and by stimulating erythropoiesis in their spleens.

These data are consistent with other studies where IDR peptides have acted in a multifaceted manner independent of direct antimicrobial activities (15, 16). The broad anti-inflammatory action appears to require rapid systemic or vascular access to PBMCs because IDR-1018 was protective against ECM only when administered intravenously, whereas the anti-infective activity against S. aureus occurred after intraperitoneal injection. Because inflammation is a major cause of morbidity in infections, IDR peptides also offer great promise for adjunctive treatment of infections. Exploring the use of protease-resistant derivatives, such as D-amino acid–containing peptides or peptidomimetics, or liposomally formulated peptides, is expected to increase drug stability and decrease the therapeutically effective dose.

In summary, the focus on adjunctive treatment in combination with first-line antimalarials and the use of advanced bioinformatic tools and network analysis allowed us to use the P. berghei ANKA model of ECM as a preclinical screen to establish the value of an interesting new class of anti-inflammatory drugs.

MATERIALS AND METHODS

Animals and parasites
Female 8-week-old C57BL/6 and BALB/c mice were purchased from the Animal Resource Centre or the Center for Disease Modeling (University of British Columbia) and maintained under conventional or specific pathogen–free conditions, respectively. Using BALB/c mice as parasite donors, we injected C57BL/6 mice intraperitoneally with 1×10^5 P. berghei ANKA–infected erythrocytes. Animals were checked several times daily for mortality and the development of neurological symptoms indicative of ECM, such as ataxia, loss of reflex, and hemiplegia. All ECM experiments were terminated 14 days after infection. All experiments were approved by the Walter and Eliza Hall Institute Animal Ethics Committee.

Peptide administration and drug treatment
The IDR-1018 and IDR-1 peptides were injected either intraperitoneally or intravenously at 8 and 24 mg/kg, respectively, in 200 μl of saline. Control mice were injected with 200 μl of saline. For antiparasitic drug treatment, pyrimethamine (70 mg/liter) (Sigma-Aldrich) and chloroquine (600 mg/liter) (diphosphate salt, Sigma-Aldrich) were administered in drinking water for 7 days. Pyrimethamine was dissolved in

dimethyl sulfoxide for a stock solution of 7 mg/ml and diluted 100-fold in water. Chloroquine was dissolved in pyrimethamine-water and adjusted to pH 5 to 6.

Transcriptional signature for ECM

From three published brain microarray data sets from early time points of *P. berghei* ANKA infection in ECM-susceptible mice (*19–21*), the following data were extracted: From Delahaye *et al.* (*20*), we used genes differentially regulated in ECM-susceptible CBA/J and/or C57BL/6 mice compared to ECM-resistant BALB/c mice (corrected for strain-specific gene expression in uninfected mice) on days 2 and 5 of infection, or on day 5 but not on day 2. From Miu *et al.* (*21*), we selected Affymetrix probes differentially expressed in CBA/T6J brains on day 6 of infection compared to uninfected controls. From Sexton *et al.* (*19*), we selected genes that were differentially expressed on day 3 of infection in C57BL/6 mice compared to uninfected controls. Microarray probes were matched across platforms by gene symbol. The combined ECM gene set of 224 up-regulated genes and 59 down-regulated genes is listed in table S1.

This consensus gene set was used to represent a transcriptional signature of ECM. The directional behavior of this signature was assessed in the microarray expression profiles with rotation gene set testing (ROAST) (*22*). This approach uses the same linear model framework as the gene-wise analyses in the limma software package. Unsupervised multidimensional scaling plots were created with the plotMDS function of the limma package, with distances defined by the leading 500-fold changes between each pair of samples. Supervised plots discriminating infected from uninfected mice used the regularized linear discriminant function method of the limma package. This function uses an empirical Bayes strategy to avoid indeterminacy of the between-gene co-variance matrix when forming the discriminant functions. In both cases, batch effects were removed before plotting by the removeBatchEffects function.

Network analysis

Pathway, Gene Ontology, and network analyses were performed with InnateDB [http://www.innatedb.com (*43*, *44*)] and Ingenuity Pathways Analysis (IPA) (http://www.ingenuity.com) after mapping Illumina probe IDs to National Center for Biotechnology Information (NCBI) RefSeq IDs. Where multiple microarray probes mapped to the same RefSeq ID, the most significant probe was chosen in IPA, whereas InnateDB calculated the average value. In InnateDB, we identified pathways significantly associated with up- and down-regulated genes using the hypergeometric algorithm, and differentially expressed mouse genes were mapped to human Ensembl IDs with InnateDB Ortholuge orthology predictions (*45*). In IPA, network analysis was run first without restrictions and then limiting the gene interactions to those published for cells of immune origin and the spleen. Networks are based on the gene interactions stored in the Ingenuity Knowledge Database and were edited to reduce the number of nondifferentially expressed intermediate genes and restricted to gene subsets with functional relevance.

BMDM differentiation and stimulation

Mouse BMDMs were prepared by culturing bone marrow cells from C57BL/6J mice for 7 days in high-glucose Dulbecco's modified Eagle's medium with 20% horse serum, 2 mM L-glutamine, 1 mM sodium pyruvate (all from Invitrogen), penicillin (50 U/ml), and streptomycin (50 μg/ml), and supplemented with 30% L-conditioned medium [supernatant of cell line L-929 transfected with a macrophage colony-stimulating factor (M-CSF) expression vector]. On day 7, cells were harvested, washed, and resuspended at 5×10^5 cells/ml in 96-well plates to rest overnight. On day 8, BMDMs were stimulated with or without IDR-1018 (100 μg/ml) with different TLR agonists: LPS (100 ng/ml) (isolated from *Pseudomonas aeruginosa* strain H103), synthetic tripalmitoylated lipopeptide (100 ng/ml) (PAM3CSK4; Invivogen), CpG 2395 (20 μg/ml) (Invivogen), and IFN-γ (10 ng/ml) (ImmunoTools). Splenocyte stimulation was performed comparably except that undifferentiated BALB/c splenocytes and CpG 2395 (10 μg/ml) were used. These experiments were approved by the University of British Columbia Animal Care Committee.

Statistical analyses

The probability of survival for mice with ECM was modeled with logistic regression to test for differences between groups while adjusting for any possible batch effects between independent experiments. One-sided likelihood score tests were conducted with the glm.scoretest function of the StatMod software package (http://www.r-project.org). Because we were only interested in protective outcomes of IDR treatment, one-sided tests were undertaken of the null hypothesis that the probability of survival of mice with ECM was equal or lower after administration of IDR peptides compared to administration of saline against the alternative hypothesis that survival was improved. To check that the asymptotic distributional assumptions of the score tests were satisfactory, we also conducted Fisher-Boschloo-Berger tests of the same hypotheses (*46*). These gave similar results, so only logistic regression score tests are reported. Parasitemias and reticulocyte counts were compared by unpaired, two-tailed Mann-Whitney tests and cytokine production by unpaired, two-tailed *t* test with Welch's correction.

SUPPLEMENTARY MATERIALS

REFERENCES AND NOTES

1. J. Golenser, J. McQuillan, L. Hee, A. J. Mitchell, N. H. Hunt, Conventional and experimental treatment of cerebral malaria. *Int. J. Parasitol.* **36**, 583–593 (2006).
2. N. J. White, G. D. Turner, I. M. Medana, A. M. Dondorp, N. P. Day, The murine cerebral malaria phenomenon. *Trends Parasitol.* **26**, 11–15 (2010).
3. J. B. de Souza, J. C. Hafalla, E. M. Riley, K. N. Couper, Cerebral malaria: Why experimental murine models are required to understand the pathogenesis of disease. *Parasitology* **137**, 755–772 (2010).
4. E. M. Riley, K. N. Couper, H. Helmby, J. C. Hafalla, J. B. de Souza, J. Langhorne, W. B. Jarra, F. Zavala, Neuropathogenesis of human and murine malaria. *Trends Parasitol.* **26**, 277–278 (2010).
5. L. Rénia, A. C. Grüner, G. Snounou, Cerebral malaria: In praise of epistemes. *Trends Parasitol.* **26**, 275–277 (2010).
6. N. H. Hunt, G. E. Grau, C. Engwerda, S. R. Barnum, H. van der Heyde, D. S. Hansen, L. Schofield, J. Golenser, Murine cerebral malaria: The whole story. *Trends Parasitol.* **26**, 272–274 (2010).
7. L. J. Carvalho, Murine cerebral malaria: How far from human cerebral malaria? *Trends Parasitol.* **26**, 271–272 (2010).
8. J. Langhorne, P. Buffet, M. Galinski, M. Good, J. Harty, D. Leroy, M. M. Mota, E. Pasini, L. Renia, E. Riley, M. Stins, P. Duffy, The relevance of non-human primate and rodent malaria models for humans. *Malar. J.* **10**, 23 (2011).

9. I. A. Clark, W. B. Cowden, Roles of TNF in malaria and other parasitic infections. *Immunol. Ser.* **56**, 365–407 (1992).

10. I. A. Clark, W. B. Cowden, G. A. Butcher, N. H. Hunt, Possible roles of tumor necrosis factor in the pathology of malaria. *Am. J. Pathol.* **129**, 192–199 (1987).

11. H. Brown, G. Turner, S. Rogerson, M. Tembo, J. Mwenechanya, M. Molyneux, T. Taylor, Cytokine expression in the brain in human cerebral malaria. *J. Infect. Dis.* **180**, 1742–1746 (1999).

12. L. Schofield, G. E. Grau, Immunological processes in malaria pathogenesis. *Nat. Rev. Immunol.* **5**, 722–735 (2005).

13. C. C. John, A. Panoskaltsis-Mortari, R. O. Opoka, G. S. Park, P. J. Orchard, A. M. Jurek, R. Idro, J. Byarugaba, M. J. Boivin, Cerebrospinal fluid cytokine levels and cognitive impairment in cerebral malaria. *Am. J. Trop. Med. Hyg.* **78**, 198–205 (2008).

14. F. Verra, V. D. Mangano, D. Modiano, Genetics of susceptibility to *Plasmodium falciparum*: From classical malaria resistance genes towards genome-wide association studies. *Parasite Immunol.* **31**, 234–253 (2009).

15. A. Nijnik, L. Madera, S. Ma, M. Waldbrook, M. R. Elliott, D. M. Easton, M. L. Mayer, S. C. Mullaly, J. Kindrachuk, H. Jenssen, R. E. W. Hancock, Synthetic cationic peptide IDR-1002 provides protection against bacterial infections through chemokine induction and enhanced leukocyte recruitment. *J. Immunol.* **184**, 2539–2550 (2010).

16. M. G. Scott, E. Dullaghan, N. Mookherjee, C. Glavas, M. Waldbrook, A. Thompson, A. Wang, K. Lee, S. Doria, P. Hamill, J. J. Yu, Y. Li, O. Donini, M. M. Guarna, B. B. Finlay, J. R. North, R. E. W. Hancock, An anti-infective peptide that selectively modulates the innate immune response. *Nat. Biotechnol.* **25**, 465–472 (2007).

17. M. Wieczorek, H. Jenssen, J. Kindrachuk, W. R. Scott, M. Elliott, K. Hilpert, J. T. Cheng, R. E. W. Hancock, S. K. Straus, Structural studies of a peptide with immune modulating and direct antimicrobial activity. *Chem. Biol.* **17**, 970–980 (2010).

18. J. Kindrachuk, H. Jenssen, M. Elliott, R. Townsend, A. Nijnik, S. F. Lee, V. Gerdts, L. A. Babiuk, S. A. Halperin, R. E. W. Hancock, A novel vaccine adjuvant comprised of a synthetic innate defence regulator peptide and CpG oligonucleotide links innate and adaptive immunity. *Vaccine* **27**, 4662–4671 (2009).

19. A. C. Sexton, R. T. Good, D. S. Hansen, M. C. D'Ombrain, L. Buckingham, K. Simpson, L. Schofield, Transcriptional profiling reveals suppressed erythropoiesis, up-regulated glycolysis, and interferon-associated responses in murine malaria. *J. Infect. Dis.* **189**, 1245–1256 (2004).

20. N. F. Delahaye, N. Coltel, D. Puthier, M. Barbier, P. Benech, F. Joly, F. A. Iraqi, G. E. Grau, C. Nguyen, P. Rihet, Gene expression analysis reveals early changes in several molecular pathways in cerebral malaria-susceptible mice versus cerebral malaria-resistant mice. *BMC Genomics* **8**, 452 (2007).

21. J. Miu, N. H. Hunt, H. J. Ball, Predominance of interferon-related responses in the brain during murine malaria, as identified by microarray analysis. *Infect. Immun.* **76**, 1812–1824 (2008).

22. D. Wu, E. Lim, F. Vaillant, M. L. Asselin-Labat, J. E. Visvader, G. K. Smyth, ROAST: Rotation gene set tests for complex microarray experiments. *Bioinformatics* **26**, 2176–2182 (2010).

23. A. T. Yeung, S. L. Gellatly, R. E. W. Hancock, Multifunctional cationic host defence peptides and their clinical applications. *Cell. Mol. Life Sci.* **68**, 2161–2176 (2011).

24. L. Rénia, S. M. Potter, M. Mauduit, D. S. Rosa, M. Kayibanda, J. C. Deschemin, G. Snounou, A. C. Grüner, Pathogenic T cells in cerebral malaria. *Int. J. Parasitol.* **36**, 547–554 (2006).

25. C. Q. Nie, N. J. Bernard, M. U. Norman, F. H. Amante, R. J. Lundie, B. S. Crabb, W. R. Heath, C. R. Engwerda, M. J. Hickey, L. Schofield, D. S. Hansen, IP-10–mediated T cell homing promotes cerebral inflammation over splenic immunity to malaria infection. *PLoS Pathog.* **5**, e1000369 (2009).

26. C. C. John, R. Opika-Opoka, J. Byarugaba, R. Idro, M. J. Boivin, Low levels of RANTES are associated with mortality in children with cerebral malaria. *J. Infect. Dis.* **194**, 837–845 (2006).

27. G. E. Grau, H. Heremans, P. F. Piguet, P. Pointaire, P. H. Lambert, A. Billiau, P. Vassalli, Monoclonal antibody against interferon γ can prevent experimental cerebral malaria and its associated overproduction of tumor necrosis factor. *Proc. Natl. Acad. Sci. U.S.A.* **86**, 5572–5574 (1989).

28. O. Koch, A. Awomoyi, S. Usen, M. Jallow, A. Richardson, J. Hull, M. Pinder, M. Newport, D. Kwiatkowski, *IFNGR1* gene promoter polymorphisms and susceptibility to cerebral malaria. *J. Infect. Dis.* **185**, 1684–1687 (2002).

29. G. E. Grau, T. E. Taylor, M. E. Molyneux, J. J. Wirima, P. Vassalli, M. Hommel, P. H. Lambert, Tumor necrosis factor and disease severity in children with falciparum malaria. *N. Engl. J. Med.* **320**, 1586–1591 (1989).

30. M. E. Molyneux, T. E. Taylor, J. J. Wirima, G. E. Grau, Tumour necrosis factor, interleukin-6, and malaria. *Lancet* **337**, 1098 (1991).

31. N. Shaffer, G. E. Grau, K. Hedberg, F. Davachi, B. Lyamba, A. W. Hightower, J. G. Breman, N. D. Phuc, Tumor necrosis factor and severe malaria. *J. Infect. Dis.* **163**, 96–101 (1991).

32. C. R. Engwerda, T. L. Mynott, S. Sawhney, J. B. De Souza, Q. D. Bickle, P. M. Kaye, Locally up-regulated lymphotoxin α, not systemic tumor necrosis factor α, is the principle mediator of murine cerebral malaria. *J. Exp. Med.* **195**, 1371–1377 (2002).

33. M. B. van Hensbroek, A. Palmer, E. Onyiorah, G. Schneider, S. Jaffar, G. Dolan, H. Memming, J. Frenkel, G. Enwere, S. Bennett, D. Kwiatkowski, B. Greenwood, The effect of a monoclonal antibody to tumor necrosis factor on survival from childhood cerebral malaria. *J. Infect. Dis.* **174**, 1091–1097 (1996).

34. M. C. D'Ombrain, D. S. Hansen, K. M. Simpson, L. Schofield, γδ-T cells expressing NK receptors predominate over NK cells and conventional T cells in the innate IFN-γ response to *Plasmodium falciparum* malaria. *Eur. J. Immunol.* **37**, 1864–1873 (2007).

35. L. J. Robinson, M. C. D'Ombrain, D. I. Stanisic, J. Taraika, N. Bernard, J. S. Richards, J. G. Beeson, L. Tavul, P. Michon, I. Mueller, L. Schofield, Cellular tumor necrosis factor, γ interferon, and interleukin-6 responses as correlates of immunity and risk of clinical *Plasmodium falciparum* malaria in children from Papua New Guinea. *Infect. Immun.* **77**, 3033–3043 (2009).

36. G. A. Awandare, B. Goka, P. Boeuf, J. K. Tetteh, J. A. Kurtzhals, C. Behr, B. D. Akanmori, Increased levels of inflammatory mediators in children with severe *Plasmodium falciparum* malaria with respiratory distress. *J. Infect. Dis.* **194**, 1438–1446 (2006).

37. D. O. Ochiel, G. A. Awandare, C. C. Keller, J. B. Hittner, P. G. Kremsner, J. B. Weinberg, D. J. Perkins, Differential regulation of β-chemokines in children with *Plasmodium falciparum* malaria. *Infect. Immun.* **73**, 4190–4197 (2005).

38. E. Belnoue, S. M. Potter, D. S. Rosa, M. Mauduit, A. C. Gruner, M. Kayibanda, A. J. Mitchell, N. H. Hunt, L. Renia, Control of pathogenic CD8+ T cell migration to the brain by IFN-γ during experimental cerebral malaria. *Parasite Immunol.* **30**, 544–553 (2008).

39. M. Nairz, A. Schroll, A. R. Moschen, T. Sonnweber, M. Theurl, I. Theurl, N. Taub, C. Jamnig, D. Neurauter, L. A. Huber, H. Tilg, P. L. Moser, G. Weiss, Erythropoietin contrastingly affects bacterial infection and experimental colitis by inhibiting nuclear factor–κB–inducible immune pathways. *Immunity* **34**, 61–74 (2011).

40. K. Kaiser, A. Texier, J. Ferrandiz, A. Buguet, A. Meiller, C. Latour, F. Peyron, R. Cespuglio, S. Picot, Recombinant human erythropoietin prevents the death of mice during cerebral malaria. *J. Infect. Dis.* **193**, 987–995 (2006).

41. L. Wiese, C. Hempel, M. Penkowa, N. Kirkby, J. A. Kurtzhals, Recombinant human erythropoietin increases survival and reduces neuronal apoptosis in a murine model of cerebral malaria. *Malar. J.* **7**, 3 (2008).

42. C. Casals-Pascual, R. Idro, N. Gicheru, S. Gwer, B. Kitsao, E. Gitau, R. Mwakesi, D. J. Roberts, C. R. Newton, High levels of erythropoietin are associated with protection against neurological sequelae in African children with cerebral malaria. *Proc. Natl. Acad. Sci. U.S.A.* **105**, 2634–2639 (2008).

43. D. J. Lynn, G. L. Winsor, C. Chan, N. Richard, M. R. Laird, A. Barsky, J. L. Gardy, F. M. Roche, T. H. Chan, N. Shah, R. Lo, M. Naseer, J. Que, M. Yau, M. Acab, D. Tulpan, M. D. Whiteside, A. Chikatamarla, B. Mah, T. Munzner, K. Hokamp, R. E. W. Hancock, F. S. Brinkman, InnateDB: Facilitating systems-level analyses of the mammalian innate immune response. *Mol. Syst. Biol.* **4**, 218 (2008).

44. D. J. Lynn, C. Chan, M. Naseer, M. Yau, R. Lo, A. Sribnaia, G. Ring, J. Que, K. Wee, G. L. Winsor, M. R. Laird, K. Breuer, A. K. Foroushani, F. S. Brinkman, R. E. W. Hancock, Curating the innate immunity interactome. *BMC Syst. Biol.* **4**, 117 (2010).

45. D. L. Fulton, Y. Y. Li, M. R. Laird, B. G. Horsman, F. M. Roche, F. S. Brinkman, Improving the specificity of high-throughput ortholog prediction. *BMC Bioinformatics* **7**, 270 (2006).

46. R. L. Berger, D. D. Boos, *P* values maximized over a confidence set for the nuisance parameter. *J. Am. Stat. Assoc.* **89**, 1012–1016 (1994).

47. M. Kanehisa, S. Goto, KEGG: Kyoto Encyclopedia of Genes and Genomes. *Nucleic Acids Res.* **28**, 27–30 (2000).

48. M. Kanehisa, S. Goto, Y. Sato, M. Furumichi, M. Tanabe, KEGG for integration and interpretation of large-scale molecular data sets. *Nucleic Acids Res.* **40**, D109–D114 (2012).

49. N. Mookherjee, P. Hamill, J. Gardy, D. Blimkie, R. Falsafi, A. Chikatamarla, D. J. Arenillas, S. Doria, T. R. Kollmann, R. E. Hancock, Systems biology evaluation of immune responses induced by human host defence peptide LL-37 in mononuclear cells. *Mol. Biosyst.* **5**, 483–496 (2009).

50. G. K. Smyth, Limma: Linear models for microarray data, in *Bioinformatics and Computational Biology Solutions Using R and Bioconductor*, R. Gentleman, V. Carey, S. Dudoit, R. Irizarry, W. Huber, Eds. (Springer, New York, 2008), pp. 397–420.

51. R. C. Gentleman, V. J. Carey, D. M. Bates, B. Bolstad, M. Dettling, S. Dudoit, B. Ellis, L. Gautier, Y. Ge, J. Gentry, K. Hornik, T. Hothorn, W. Huber, S. Iacus, R. Irizarry, F. Leisch, C. Li, M. Maechler, A. J. Rossini, G. Sawitzki, C. Smith, G. Smyth, L. Tierney, J. Y. Yang, J. Zhang, Bioconductor: Open software development for computational biology and bioinformatics. *Genome Biol.* **5**, R80 (2004).

52. W. Shi, A. Oshlack, G. K. Smyth, Optimizing the noise versus bias trade-off for Illumina whole genome expression BeadChips. *Nucleic Acids Res.* **38**, e204 (2010).

53. G. K. Smyth, Linear models and empirical Bayes methods for assessing differential expression in microarray experiments. *Stat. Appl. Genet. Mol. Biol.* **3**, Article3 (2004).

54. Y. Benjamini, Y. Hochberg, Controlling the false discovery rate: A practical and powerful approach to multiple testing. *J. R. Statist. Soc. Ser. B* **57**, 289–300 (1995).

55. B. M. Bolstad, R. A. Irizarry, M. Astrand, T. P. Speed, A comparison of normalization methods for high density oligonucleotide array data based on variance and bias. *Bioinformatics* **19**, 185–193 (2003).

56. M. L. Mayer, J. A. Sheridan, C. J. Blohmke, S. E. Turvey, R. E. Hancock, The *Pseudomonas aeruginosa* autoinducer 3O-C12 homoserine lactone provokes hyperinflammatory responses from cystic fibrosis airway epithelial cells. *PLoS One* **6**, e16246 (2011).

57. O. M. Pena, J. Pistolic, D. Raj, C. D. Fjell, R. E. Hancock, Endotoxin tolerance represents a distinctive state of alternative polarization (M2) in human mononuclear cells. *J. Immunol.* **186**, 7243–7254 (2011).

58. M. E. Smoot, K. Ono, J. Ruscheinski, P. L. Wang, T. Ideker, Cytoscape 2.8: New features for data integration and network visualization. *Bioinformatics* **27**, 431–432 (2011).

59. M. S. Cline, M. Smoot, E. Cerami, A. Kuchinsky, N. Landys, C. Workman, R. Christmas, I. Avila-Campilo, M. Creech, B. Gross, K. Hanspers, R. Isserlin, R. Kelley, S. Killcoyne, S. Lotia, S. Maere, J. Morris, K. Ono, V. Pavlovic, A. R. Pico, A. Vailaya, P. L. Wang, A. Adler, B. R. Conklin, L. Hood, M. Kuiper, C. Sander, I. Schmulevich, B. Schwikowski, G. J. Warner, T. Ideker, G. D. Bader, Integration of biological networks and gene expression data using Cytoscape. *Nat. Protoc.* **2**, 2366–2382 (2007).

60. C. Y. Lin, C. H. Chin, H. H. Wu, S. H. Chen, C. W. Ho, M. T. Ko, Hubba: Hub objects analyzer—A framework of interactome hubs identification for network biology. *Nucleic Acids Res.* **36**, W438–W443 (2008).

61. D. M. Bowdish, D. J. Davidson, M. G. Scott, R. E. W. Hancock, Immunomodulatory activities of small host defense peptides. *Antimicrob. Agents Chemother.* **49**, 1727–1732 (2005).

Citation: A. H. Achtman, S. Pilat, C. W. Law, D. J. Lynn, L. Janot, M. L. Mayer, S. Ma, J. Kindrachuk, B. B. Finlay, F. S. L. Brinkman, G. K. Smyth, R. E. W. Hancock, L. Schofield, Effective adjunctive therapy by an innate defense regulatory peptide in a preclinical model of severe malaria. *Sci. Transl. Med.* **4**, 135ra64 (2012).